The stability of Au-chloride complexes in water vapor at elevated temperatures and pressures

Article *in* Geochimica et Cosmochimica Acta · December 2001

DOI: 10.1016/S0016-7037(01)00730-X

3 authors:

Sandy Archibald
Aurum Exploration Services
15 PUBLICATIONS 342 CITATIONS
SEE PROFILE

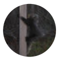

Artas Migdisov
Los Alamos National Laboratory
101 PUBLICATIONS 2,978 CITATIONS
SEE PROFILE

Anthony E. Williams-Jones
McGill University
346 PUBLICATIONS 10,659 CITATIONS
SEE PROFILE

Pergamon

Geochimica et Cosmochimica Acta, Vol. 65, No. 23, pp. 4413–4423, 2001

0016-7037/01 \$20.00 + .00

PII S0016-7037(00)00730-X

The stability of Au-chloride complexes in water vapor at elevated temperatures and pressures

S. M. ARCHIBALD, A. A. MIGDISOV, and A. E. WILLIAMS-JONES
Department of Earth and Planetary Sciences, McGill University, 3450 University Street, Montreal, Quebec, H3A 2A7, Canada

(*Received February* 13, 2001; *accepted in revised form June* 19, 2001)

Abstract—The solubility of gold in liquid-undersaturated HCl-bearing water vapor was investigated experimentally at temperatures of 300 to 360°C and pressures up to 144 bars. Results of these experiments show that the solubility of gold in the vapor phase is significant and increases with increasing f_{HCl} and f_{H_2O}. This behavior of gold is attributed to formation of hydrated gold–chloride gas species, interpreted to have a gold–chlorine ratio of 1:1 and a hydration number varying from 5 at 300°C to 3 at 360°C. These complexes are proposed to have formed through the following reaction:

$$Au^{solid} + m \cdot HCl^{gas} + n \cdot H_2O^{gas} = AuCl_m \cdot (H_2O)_n^{gas} + \frac{m}{2} \cdot H_2^{gas}, \qquad (A1)$$

which was determined to have log K values of −17.28 ± 0.36 at 300°C, −18.73 ± 0.66 at 340°C, and −18.74 ± 0.43 at 360°C. Gold solubility in the vapor was retrograde, i.e., it decreased with increasing temperature, possibly as a result of the inferred decrease in hydration number.

Calculations based on our data indicate that at 300°C and f_{O_2}-pH conditions, encountered in high sulfidation epithermal systems, the vapor phase can transport up to 6.6 ppb gold, which would be sufficient to form an economic deposit (e.g., Nansatsu, Japan; 36 tonnes) in ~ 30,000 yr. *Copyright © 2001 Elsevier Science Ltd*

1. INTRODUCTION

The widespread occurrence of boiling in hydrothermal systems has led a number of researchers to suggest that the vapor phase may play an important role in the transport of ore metals (Drummond and Ohmoto, 1985; Hedenquist and Lowenstern, 1994; Hedenquist, 1995; Migdisov et al., 1999). Until recently, the most convincing evidence for this has come from active volcanoes, where a variety of metals have been detected in gas condensates and fumarolic encrustations. The highest reported gold concentration in a volcanic gas condensate is 24 ppb, which was determined for high-temperature fumarolic gases collected at Momotombo volcano in Nicaragua (Gemmell, 1987). More typically, gold concentrations in volcanic gas condensates are <1 ppb, but even at this level, they can sublimate gold. For example, Taran et al. (2000) documented the presence of native gold among sublimates collected in a silica tube experiment at Colima volcano in Mexico, where the gold concentration in gas condensates was between 0.1 and 0.5 ppb. Direct evidence of the transport of gold by the vapor phase in an ore-forming hydrothermal system was provided two years ago by the discovery of vapor-rich fluid inclusions in the giant Grasberg porphyry Cu-Au deposit in Indonesia, which Ulrich et al. (1999) showed contain up to 10 ppm gold (LA-ICPMS analyses). Significantly, the coexisting brine inclusions contain <0.3 ppm Au.

There have been many attempts to estimate the solubility of metals in hydrothermal vapors thermodynamically by using metal volatility data and initial fluid compositions (e.g., Symonds et al., 1987; Spycher and Reed, 1989; Symonds and Reed, 1993; Getahun et al., 1996; Taran et al., 2000). However, these estimates do not take into account the interaction between the metal component dissolved in the gas and the gas solvent. Because water is the major component of crustal gases, including those released from volcanoes (Symonds et al., 1994), it is essential that solvation (hydration) be considered when calculating the metal transportation potential of natural systems. In one of the few previous studies to investigate the role that hydration plays in the solubility of an economic metal in vapor, Migdisov et al. (1999) showed that the presence of water vapor increases the concentration of AgCl in the vapor phase by between 1.5 and 2 orders of magnitude. They postulated that the silver was dissolved as the species $AgCl \cdot (H_2O)_3$.

Considering that gold is transported predominantly as a chloride complex in high-temperature aqueous liquids (Zotov et al., 1990), and considering that HCl is an important component of volcanic gases (Symonds et al., 1994), it is likely that if gold partitions significantly into the vapor phase, it does so as a gaseous gold chloride complex. Several studies have investigated the vapor transport of gold as chloride complexes experimentally, but none have involved aqueous vapor. The earliest investigations were those of Fischer and Biltz (1928) and Biltz et al. (1928), which evaluated the relationships between gold and chloride, bromide, and iodide gases. Their studies concluded that gold–halogen complexes form at all the temperatures investigated (200 to 1200°C). Subsequent studies by Landsberg and Hoatson (1970), Hager and Hill (1970), James and Hager (1978), and Tagirov et al. (1993) focused on the $Au\text{-}Cl_2$ system and determined thermodynamic constants for the various species formed, notably Au_2Cl_6, and $AuCl_2$.

Although the $Au\text{-}Cl_2$ system is important in extractive metallurgy, it is unlikely to satisfactorily model the vapor transport of gold in a water-rich hydrothermal setting because of the potentially important role of H_2O-Au interactions. The objectives of this study are first to investigate the effect of H_2O-Au interactions on the solubility of gold in the vapor phase by

---

* Author to whom correspondence should be addressed (sandy@eps.mcgill.ca).

measuring its solubility in the system Au-H_2O-HCl, and second to evaluate the role that vapor transport might play in concentrating gold to economically exploitable levels.

2. EXPERIMENTAL METHODS

The experimental method used here is similar to that used by Migdisov et al. (1998, 1999), except that gold was introduced as the native metal rather than as the metal chloride. Experiments were conducted at temperatures between 300 and 360°C and pressures low enough to ensure that the aqueous vapor was undersaturated with respect to liquid (see Appendix, Tables A1–A3). Two types of furnace were used in the experiments. In experiments conducted at 340 and 360°C, an electric furnace (internal diameter 15 cm, height 50 cm) equipped with aluminum walls (1 cm thick) to reduce temperature gradients was used for heating. A thermal regulator allowed the temperature to be controlled to approximately ±0.5°C. Prior to each experiment; temperature gradients within the apparatus were measured by three thermocouples, located at the top, bottom, and center of the furnace. The vertical gradients were typically in the range 0.5 to 1.0°C/m. Temperatures during runs were measured with two chromel-alumel thermocouples, located in the top and bottom of the furnace. Experiments at 300°C were conducted in a Fisher Isotemp forced draft oven (model 838F). To reduce thermal gradients, the oven was modified by adding an aluminum box with 1.5-cm-thick walls to hold the autoclaves. After this modification, gradients were less than 0.5°C/m. A thermocouple placed inside the aluminum box was used to obtain an accurate reading of the internal temperature.

Experiments were performed in titanium autoclaves and involved measuring the solubility of native gold in HCl–water vapor. The autoclaves were constructed from grade 2 titanium alloy (ASTM B348) (Fig. 1). The internal surfaces of each autoclave were preconditioned with nitric acid to produce a protective layer of TiO_2. The volumes of the autoclaves ($\sim$100 cm^3) were determined by filling them with 25°C distilled water from a Teflon beaker and weighing this beaker before and after filling. The weighing was performed to an accuracy of ±0.1 g.

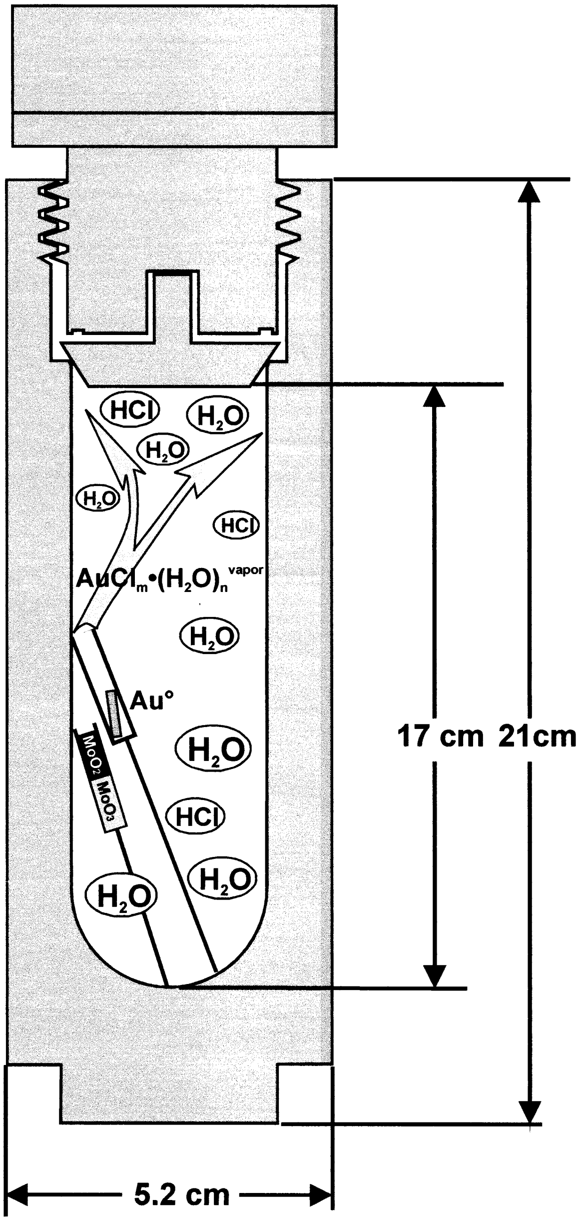

Fig. 1. A section through a titanium autoclave of the type used in this study. The autoclaves were constructed from titanium alloy (grade 2 ASTM B348).

Before each run, dry nitrogen gas was passed through the autoclaves for 10 to 20 min to remove any atmospheric gases. During experiments, autoclaves were loaded with an open quartz-glass ampoule containing native gold wire (Alfa Aesar, 99.99% purity) and a second quartz-glass ampoule containing an oxygen buffer assemblage of MoO_2-MoO_3 (Alfa Aesar, 99.95% purity). This buffer was chosen over more conventional oxygen buffers (e.g., hematite–magnetite, quartz–fayalite–magnetite, Ni-NiO) because thermodynamic calculations showed the Mo assemblage to be several orders of magnitude less soluble than assemblages containing Ni and Fe at the experimental P_{HCl}. The calculated oxygen fugacities of $-\log 21$ to $-\log 19$ (Fig. 2) over the temperature range of 300 to 360°C are higher than those in near-surface fumarole settings and in high-sulfidation systems, which are generally $< -\log 28$ and typically on the order of $\sim -\log 31$, i.e., that of the H_2S-SO_2 buffer at 300°C (Hedenquist, 1995). This value is substantially higher than those of the quartz–fayalite–magnetite and hematite–magnetite buffer, which range from -36 to -31 and -31 to -27, respectively, at temperatures of 300 and 360°C.

A known volume of HCl solution, produced by adding Optima-grade HCl to distilled, nanopure water, was placed in the bottom of the autoclave with a pipette to prevent contact of the solution with the solid Au. The volume of HCl solution placed in the autoclave corresponded to an amount that would ensure that the system was liquid-undersaturated at the experimental conditions, and any gold dissolution was entirely in the dry vapor phase. Because of the extremely low vapor pressure of gold (Tagirov et al., 1993) and HCl compared with that of water vapor, the total pressure in a run was assumed to be equal to that of pure water vapor. This pressure was calculated by using the autoclave volume and the equation of state for water of Kestin et al. (1984). The P_{HCl} of the vapor was calculated from the pH of the solution at 25°C and an assumption that 1 mol of $[H]^+$ would produce 1 mole of HCl in the gaseous phase at the temperature of investigation (Ruaya and Seward, 1987; Tagirov et al., 1997).

After each run, the autoclave was quenched rapidly by placing it in a cold-water bath and passing a stream of compressed air over it, until room temperature was reached. This normally took $\sim$15 min. The quartz-glass capsules containing the oxygen buffer and native gold were then removed from the vessel, and the condensate was transferred to a clean test tube to measure its pH. After the condensate was transferred back into the autoclave, 3 to 5 mL of aqua regia (Fisher Scientific; Optima-grade HCl and HNO_3) were added to dissolve any gold on the walls of the autoclave. The concentrations of gold dissolved in the condensates and washing solutions were determined by instrumental neutron activation analysis with a detection limit of 30 parts per trillion.

Two potential sources of experimental error are retransportation on the walls of the autoclave during runs (transport reaction) due to the temperature gradient in the oven and partitioning of Au from the vapor into the liquid (Migdisov et al., 1999). Transport reactions may produce an irreversible transfer of gold from the sample to the autoclave walls

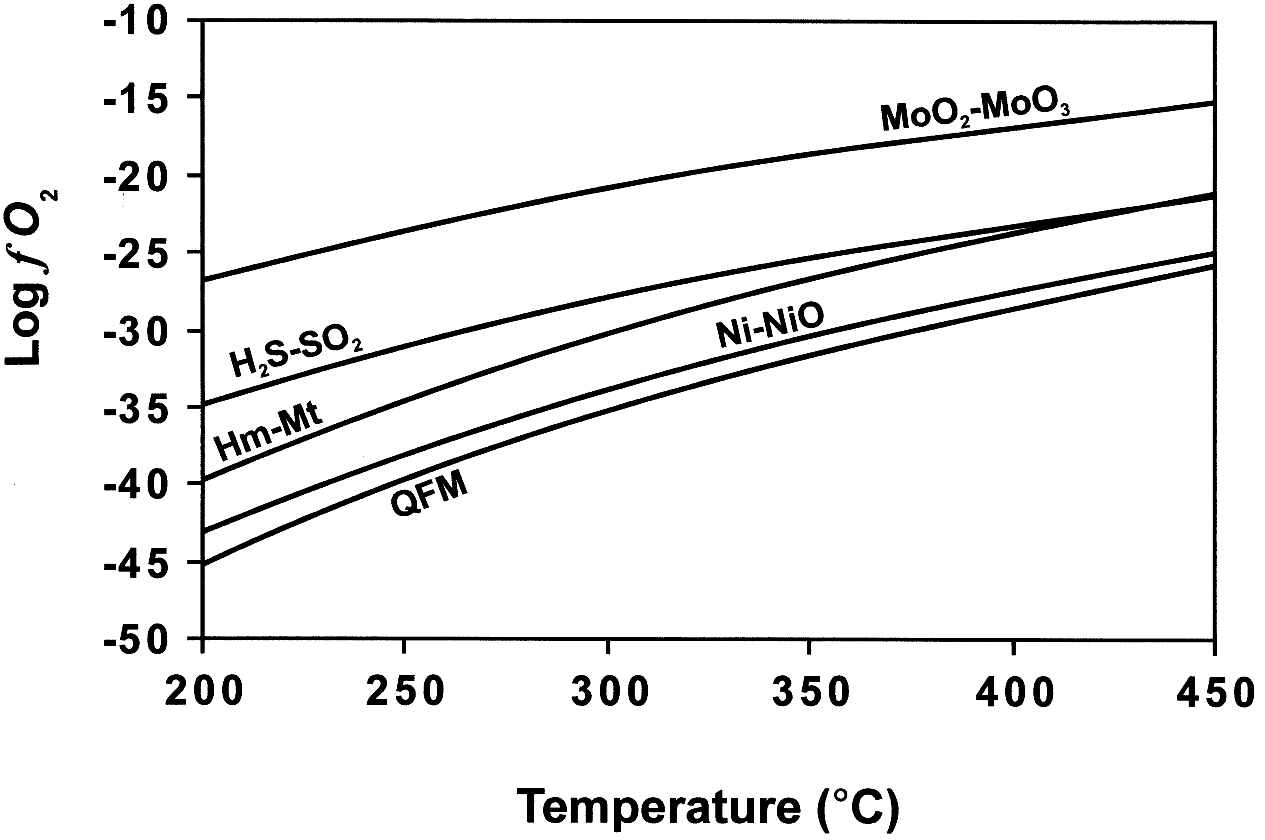

Fig. 2. A plot showing log f_{O_2} as a function of temperature for several common oxygen buffers (Hm-Mt = hematite–magnetite; QFM = quartz–fayalite–magnetite) calculated at 100 bars using internal database supplied by the thermodynamic program HCh (Shvarov and Bastrakov, 1999). The fugacity of oxygen in our experiments was buffered by the assemblage MoO_2-MoO_3.

during cooling, or during heating, which could lead to considerable overestimation of metal solubility in the vapor phase. The second potential source of error is partitioning of the gold from vapor into liquid (water) during heating or quenching. The much higher solubility of Au in the liquid (several orders of magnitude) could result in overestimation of the solubility in the vapor. Neither of these processes seems to have occurred during the experiments, as the kinetic runs (see below) do not show evidence of an increase in concentration with time (i.e., a transport reaction) or a scattering of concentrations (i.e., condensation).

In several cases, there was an increase in pH from the start to the finish of an experiment. This increase is interpreted to have occurred when the autoclave was cooled and to have been caused by the escape of HCl vapor due to the difference in thermal expansion of the body of the autoclave and the cover. Had leaking occurred during initial heating of the autoclave, a loss of liquid would have resulted. This loss was observed in several of the runs but was eliminated when the cover was further tightened. If large losses (e.g., >0.5 mL) of liquid were noted, the data were discarded.

3. RESULTS

A series of kinetic experiments was performed to determine the time taken to reach equilibrium and to investigate potential sources of experimental error. These experiments were conducted at 300°C under constant water pressure, close to the liquid–vapor boundary, for durations of 3 to 21 days. At this temperature, equilibrium was attained after 10 days (Fig. 3). In subsequent experiments at temperatures <320°C, autoclaves were left in the furnace for at least 12 days, whereas at higher temperatures, this time was reduced to 8 days. Figure 3 shows that once equilibrium was attained, Au solubilities were reproducible to approximately ±20%. If condensation had occurred on the inner surface of the autoclave at the run temperature, the

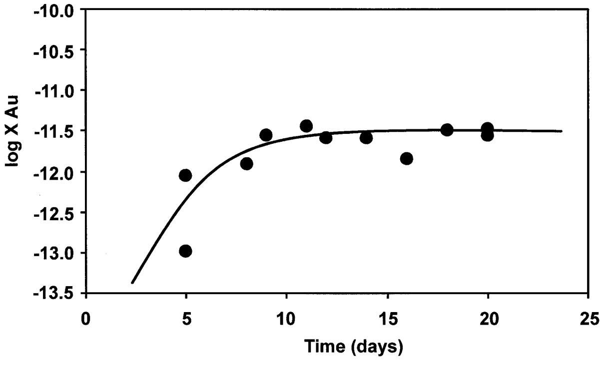

Fig. 3. The solubility of $AuCl_m \cdot (H_2O)_n$, at log $P_{HCl} = -2.72$ and log $P_{H_2O} = 1.90$ as a function of time. The data suggest that equilibrium was attained after 10 days at 300°C.

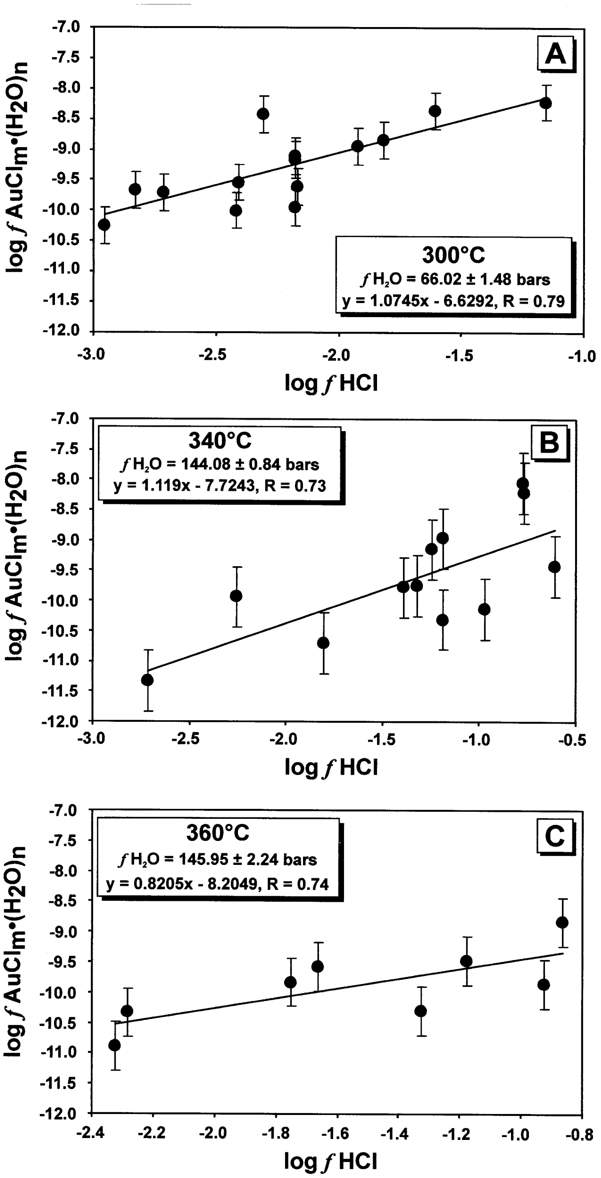

Fig. 4. Plots of values of log $f_{AuCl_m} \cdot (H_2O)_n$ vs. log f_{HCl} (constant f_{H_2O}) at three isotherms (a, 300°C; b, 340°C; c, 360°C). The slope of ~1 at these temperatures suggests the stoichiometry $AuCl \cdot (H_2O)_n$.

concentrations measured would not have been reproducible. In several runs, liquid is interpreted to have formed within the autoclave as a result of temperature fluctuations caused by furnace malfunctions. The gold concentrations in these runs were anomalously high, indicating that gold condensed (or was transported) during the experiments and the process was irreversible. The concentration measured after quenching to room temperature consisted of gold that condensed from the vapor at the end of the experiment, plus the gold transported during the runs. Results from these experiments were not used further in this investigation.

Three isotherms (300, 340, 360°C) were chosen to evaluate the solubility of gold in the vapor phase. Thirty-four experiments were conducted at constant f_{H_2O} (Figs. 4A–C) and a further 33 experiments at constant f_{HCl} (Figs. 5A–D) to investigate the effects of f_{HCl} and f_{H_2O} on gold solubility (Appendix). The vapor pressure in the Au-H_2O-HCl system varied from 27 to 113 bars and was close to that of the liquid–vapor boundary.

The results of our experiments show that gold concentration correlates positively with respect to both f_{HCl} and f_{H_2O} (Figs. 4 and 5), indicating that solubility of gold in the vapor phase depends on the fugacity of HCl, as well as the fugacity of H_2O. Our experiments also show that the solubility of gold, at similar f_{H_2O} and f_{HCl}, is retrograde over the temperature interval 300 to 360°C. In the next section, we use the data in the Appendix (Tables A1–A3) to estimate the stoichiometry of the gaseous gold species.

4. DISCUSSION

The concentration of gold in vapor increased with increasing f_{HCl} and f_{H_2O}, and it thus can be assumed that the dominant species has the stoichiometry $AuCl_m \cdot (H_2O)_n^{gas}$. An overall reaction that describes the formation of this species from the starting components is

$$Au^{gas} + m \cdot HCl^{gas} + n \cdot H_2O^{gas} = AuCl_m \cdot (H_2O)_n^{gas} + \frac{m}{2} \cdot H_2^{gas}, \tag{1}$$

where m is the chlorine ligation number, n is the hydration number of the gold species in vapor, and Au^{gas} represents the vapor pressure of Au^{gas} over Au^{solid}. This equation can also be used for nonhydrated species such as $AuCl_3$ (n = 0; m = 3).

In our study, the experimental method was designed to investigate the dependence of gold concentration on the fugacity of HCl and H_2O, and does not allow differentiation between species with the same metal–ligand ratio. (e.g., Au_2Cl_6 is indistinguishable from $AuCl_3$). We were therefore able to determine the ratio of Au:Cl, but not the stoichiometry of the dominant gold species.

4.1. Thermodynamic Interpretations

Data from our experiments were interpreted assuming that the vapor was an ideal mixture of nonideal gases (c.f., Marshall, 1972; Armellini and Tester, 1993; Migdisov et al., 1999). However, because fugacity coefficients for HCl and the gold vapor species are not available, we had to treat these gases ideally (i.e., $P_{gas} = f_{gas}$). The equilibrium constant for reaction 1 is given by

$$\log K_f = \log f_{AuCl_m \cdot (H_2O)_n} + \frac{m}{2} \cdot \log f_{H_2} - n \cdot \log f_{H_2O} - m \cdot \log f_{HCl} - \log f_{Au}. \tag{2}$$

If log K is differentiated with respect to log f_{HCl} while holding temperature, f_{O_2}, and f_{H_2O} constant, and if the equilibrium constant of a homogeneous gaseous reaction is considered to be independent of total pressure, Eqn. 2 becomes

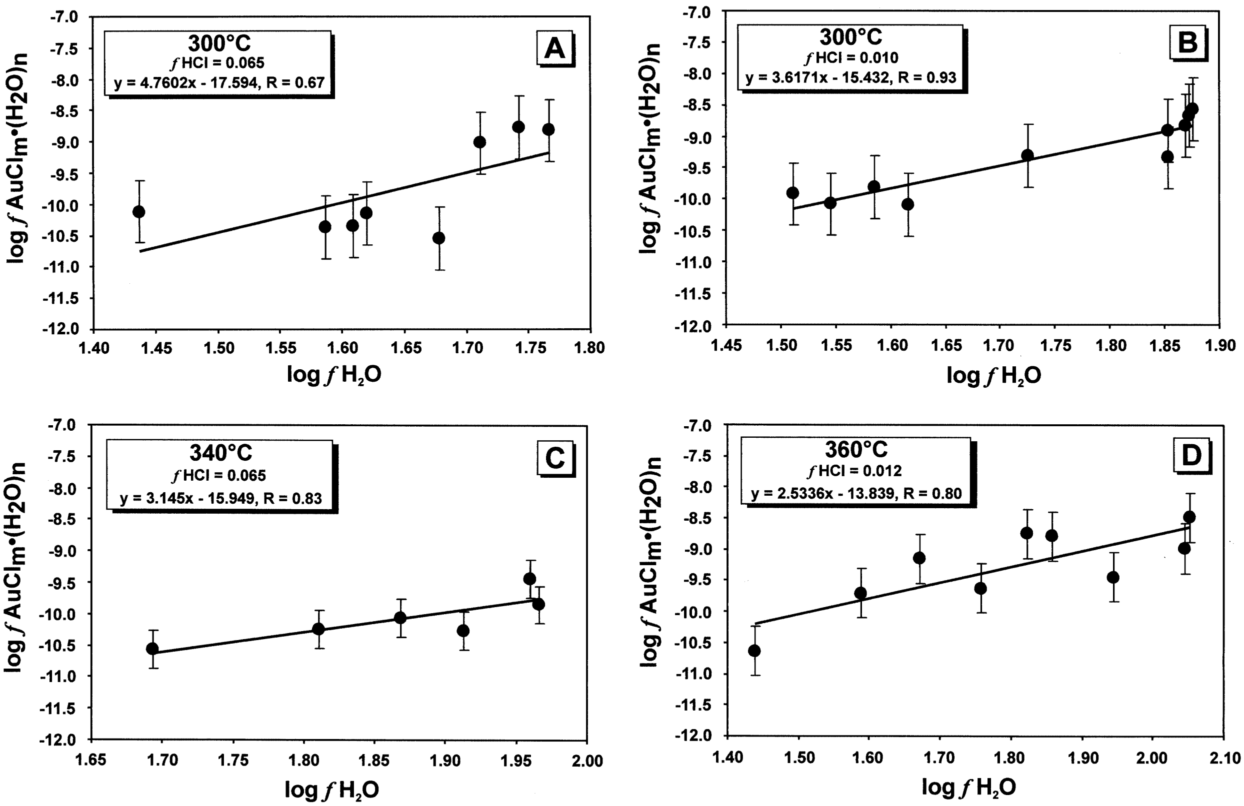

Fig. 5. Plots of values of log $f_{AuCl_m} \cdot (H_2O)_n$ vs. log f_{H_2O} (at constant f_{HCl}) at three isotherms (a and b, 300°C; c, 340°C; d, 360°C). The slopes of the graphs are 4.7 and 3.6 (300°C), 3.1 (340°C) and 2.5 (360°C), respectively. This suggests the stoichiometry to be AuCl · $(H_2O)_{5\text{-}3}$.

$$\left(\frac{\partial \log K}{\partial \log f_{HCl}}\right)_{T,f_{H_2O},f_{O_2}} = 0 = \left(\frac{\partial \log f_{AuCl(H_2O)}}{\partial \log f_{HCl}}\right)_{T...}$$
$$- m\cdot\left(\frac{\partial \log f_{HCl}}{\partial \log f_{HCl}}\right)_{T...} + \frac{m}{2}\cdot\left(\frac{\partial \log f_{H_2}}{\partial \log f_{HCl}}\right)_{T...} + \left(\frac{\partial \log f_{Au}}{\partial \log f_{HCl}}\right)_{T...} \tag{3}$$

If we assume that f_{H_2} is constant at constant f_{H_2O} and f_{O_2}, and if we assume that the dependence of f_{Au} on f_{HCl} is negligible, Eqn. 3 simplifies to

$$\left(\frac{\partial \log f_{AuCl\,(H_2O)}}{\partial \log f_{HCl}}\right)_{T,\,f_{H_2O},\,f_{O_2}} = m. \tag{4}$$

where m, the chlorine ligation number, is the slope of a trend describing the experimental data by the orthogonal coordinates, log $f_{AuCl(H_2O)}$ and log f_{HCl}.

The hydration number of the vapor species was calculated in a similar manner. Differentiating Eqn. 2 with respect to log f_{H_2O}, we obtain

$$\left(\frac{\partial \log K_r}{\partial \log f_{H_2O}}\right)_{T,f_{HCl},f_{O_2}} = 0 = \left(\frac{\partial \log f_{AuCl(H_2O)}}{\partial \log f_{H_2O}}\right)_{T...}$$
$$+ \frac{m}{2}\cdot\left(\frac{\partial \log f_{H_2}}{\partial \log f_{H_2O}}\right)_{T...} - \left(\frac{\partial \log f_{Au}}{\partial \log f_{H_2O}}\right)_{T...} - n\left(\frac{\partial \log f_{H_2O}}{\partial \log f_{H_2O}}\right)_{T...}. \tag{5}$$

This equation can be simplified as follows:

$$H_2O = H_2 + \frac{1}{2}O_2. \tag{6}$$

Thus,

$$\log f_{H_2} = \log K_{H_2O} - \frac{1}{2}\cdot \log f_{O_2} + \log f_{H_2O} \tag{7}$$

and

$$\left(\frac{\partial \log f_{H_2}}{\partial \log f_{H_2O}}\right)_{T,f_{O_2}} = \left(\frac{\partial \log K_{H_2O}}{\partial \log f_{H_2O}}\right)_{T...}$$
$$- \frac{1}{2}\cdot\left(\frac{\partial \log f_{O_2}}{\partial \log f_{H_2O}}\right)_{T...} + \left(\frac{\partial \log f_{H_2O}}{\partial \log f_{H_2O}}\right)_{T...} \tag{8}$$

or

$$\left(\frac{\partial \log f_{H_2}}{\partial \log f_{H_2O}}\right)_{T,f_{O_2}} = 0 - 0 + 1 = 1. \tag{9}$$

Substitution of Eqn. 9 into Eqn. 5 yields

Table 1. Summary of equilibrium constants derived in this study.

Temperature (°C)	Reaction	Log K (± 1 σ error)
300	$Au + HCl + 5H_2O = AuCl \cdot (H_2O)_5 + ½H_2$	-17.28 ± 0.36
340	$Au + HCl + 4H_2O = AuCl \cdot (H_2O)_4 + ½H_2$	-18.73 ± 0.66
360	$Au + HCl + 3H_2O = AuCl \cdot (H_2O)_3 + ½H_2$	-18.74 ± 0.43

$$\left(\frac{\partial \log K_r}{\partial \log f_{H_2O}}\right)_{T,f_{HCl},f_{O_2}} = 0 = \left(\frac{\partial \log f_{AuCl\,(H_2O)}}{\partial \log f_{H_2O}}\right)_{T...} + \frac{m}{2} - \left(\frac{\partial \log f_{Au}}{\partial \log f_{H_2O}}\right)_{T...} - n \cdot \left(\frac{\partial \log f_{H_2O}}{\partial \log f_{H_2O}}\right)_{T...}. \quad (10)$$

Thus,

$$\left(\frac{\partial \log f_{AuCl\,(H_2O)}}{\partial \log f_{H_2O}}\right)_{T,f_{HCl},f_{O_2}} = n - \frac{m}{2} - \left(\frac{\partial \log f_{Au^{gas}}}{\partial \log f_{H_2O}}\right)_{T...}. \quad (11)$$

Because the system investigated was not homogeneous (i.e., it contained both solid and vapor), we applied a "Poynting correction" to make it effectively homogeneous for the purpose of thermodynamic description (Sandler, 1989, p. 225). This involved correcting the change in the pressure of Au^{gas} over the crystalline phase from that for a total pressure of $P_1 = 1$ bar (standard state) to that for P_2, the pressure of the run:

$$\ln\frac{f_2^o}{f_1^o} = \int_{P_1}^{P_2} \frac{V^0}{R \cdot T}\, dP. \quad (12)$$

Because changes in the molar volume of the native gold with temperature are negligible at the experimental temperatures (300, 340, 360°C), it was assumed that V^o is constant and that Eqn. 12 can therefore be expressed as

$$\ln\frac{f_2^o}{f_1^o} = \frac{V^o \cdot (P_2 - P)_1}{R \cdot T}, \quad (13)$$

where V^o is the molar volume (10.216 $cm^3\ mol^{-1}$ for Au; Robie, 1966) and f_1^o and f_2^o are the pressures of this component in states 1 and 2.

Substituting Eqn. 13 into Eqn. 11, we obtain

$$\left(\frac{\partial \log f_{AuCl\,(H_2O)}}{\partial \log f_{H_2O}}\right)_{T,f_{HCl},f_{O_2}} = n - \frac{m}{2} - \left(\frac{V^o \cdot (P_2 - P)_1}{R \cdot T}\right). \quad (14)$$

4.2. Data Analysis

In our calculations, we assumed that f_{HCl} was negligible compared with f_{H_2O}. The values of f_{H_2O} were calculated from the equation of Kestin et al. (1984), whereas the fugacity of $AuCl_m \cdot (H_2O)_n$ in vapor was calculated from the concentration of gold in quenched condensate (Table 2). The mole fraction of gold is therefore given by the equation,

$$X_{AuCl_m \cdot (H_2O)_n} \equiv \left(\frac{M_{AuCl_m \cdot (H_2O)_n}}{M_{H_2O}}\right), \quad (15)$$

where M is the number of moles of the corresponding compound in 1000 g of H_2O, and for an ideal mixture,

$$X_{AuCl_m \cdot (H_2O)_n} = \frac{f_{AuCl_m \cdot (H_2O)_n}}{f_{H_2O}}. \quad (16)$$

The results of the thermodynamic interpretations are presented in the Appendix and express the concentrations of the gold species as mole fractions and fugacities. Values of log $f_{AuCl_m} \cdot (H_2O)_n$ are shown as a function of f_{HCl} at 300, 340, and 360°C in Figures 4A, B, and C, respectively, and within experimental error, they correlate positively. The slope of a linear regression through the data at 300°C and an f_{H_2O} of 66 bars is 1.1 (Fig. 4A). The same slope (1.1) was obtained for a temperature of 340°C and 144 bars of pressure (Fig. 4B), whereas that for 360°C is 0.8 at a fugacity of 146 bars (Fig. 4C). These three gradients of ~1 indicate that there was one dominant gaseous gold species over the range of temperatures investigated and that it had a stoichiometry Au:Cl = 1:1 (i.e., $AuCl \cdot (H_2O)_n$).

The hydration number of the proposed vapor species $AuCl \cdot (H_2O)_n$ was interpreted from the variation of log $f_{AuCl_m \cdot (H_2O)_n}$ with log f_{H_2O} at constant log f_{HCl} (as in Eqn. 14). From Figure 5, it is apparent that $f_{AuCl \cdot (H_2O)_n}$ correlates positively with f_{H_2O}. The data at 300°C, which were collected for constant HCl fugacities of 65.5 and 9.7 millibars, yielded slopes of 4.7 and 3.6, respectively (Figs. 5A,B). The slope decreased to 3.1 at 340°C and a fugacity of 65.3 millibars HCl (Fig. 5C) and decreased further to 2.5 at 360°C and a fugacity of 11.8 millibars (Fig. 5D). These results correspond to a hydration number of 5.3 and 4.2 at 300°C, 3.7 at 340°C, and 2.9 at 360°C when the slopes are substituted into Eqn. 11, which may imply a mix of species with hydration numbers from 5 to 4 at 300°C, a predominance of $AuCl \cdot (H_2O)_4$ at 340°C, and $AuCl \cdot (H_2O)_3$ at 360°C.

To calculate the log K for the overall reaction (Eqn. 1), a slight modification to the equation is needed. This modification requires that the gold be in its standard state (i.e., solid). The equation now becomes

$$Au^{solid} + HCl^{gas} + n \cdot H_2O^{gas} = AuCl \cdot (H_2O)_n^{gas} + \frac{1}{2} \cdot H_2{}^{gas}. \quad (17)$$

When the fugacity of H_2 was calculated from Eqn. 6, it was assumed that H_2O was at 1 bar of pressure (i.e., in its standard state). The hydration number at 300°C was assumed to be 5. The log $K_{(17)}$ values were calculated for each of the isotherms investigated (Table 1). The equilibrium constants and errors for reaction 17 are -17.28 ± 0.36 (n = 5), -18.73 ± 0.66 (n = 4), -18.74 ± 0.43 (n = 3) at temperatures of 300, 340, and 360°C. The errors are expressed as 1σ deviations and refer only to experimental uncertainties.

The above values of log $K_{(17)}$ were used to calculate the partition coefficient between vapor ($AuCl \cdot (H_2O)_n$) and liquid (dissolved as $AuCl_2^-$) by the thermodynamic program HCh (Shvarov and Bastrakov, 1999) and the data for the $AuCl_2^-$ species from Zotov et al. (1990). The calculations produced partition coefficients (vapor phase/liquid phase) of 0.877461, 0.000779, and 0.000008 at temperatures of 300, 340, and 360°C. This suggests that gold strongly prefers the liquid phase over the vapor phase at these temperatures and at vapor-saturated pressures. Because of the variation in hydration numbers, it is not possible to extract values of fundamental thermodynamic parameters (e.g., entropy, enthalpy, and heat capacity) from the data.

4.3. Comparison with Other Studies

As noted earlier, previous experiments investigating the transport of gold in the vapor phase have been restricted to the system $Au\text{-}Cl_2$. These showed that Au_2Cl_6 is the dominant species at temperatures below 450°C (Biltz et al., 1928; Fischer and Biltz, 1928; Hager and Hill, 1970; Landsberg and Hoatson, 1970; James and Hager, 1978), whereas Au_2Cl_2 predominates at temperatures greater than 450°C (Hager and Hill, 1970; Landsberg and Hoatson, 1970; James and Hager, 1978). They also show that there is an minimum in solubility between 250 and 480°C. On the basis of thermodynamic data extracted from the results of their experiments, James and Hager (1978) calculated the partial pressure of gold in the $Au\text{-}Cl_2$ system to be 7.9×10^{-4} bars at 300°C and $P_{Cl_2} = 1$ bar. At the same temperature, this value decreased to 1.1×10^{-6} bars at $P_{Cl_2} = 0.1$ bar. With an increase in temperature (360°C), the pressure of the gold vapor species fell to 1×10^{-4} at $P_{Cl_2} = 1$ bar and 1.148×10^{-7} at $P_{Cl_2} = 0.1$ bar.

Calculations that used the thermodynamic data of James and Hager (1978) yield mole fractions for gold relative to water vapor (Au_2Cl_6) on the order of 10^{-50} to 10^{-52} for temperatures between 300 and 360°C, at log $f_{O_2} = -22$, and between 10^{-39} and 10^{-38} for the same temperatures, and log $f_{O_2} = -14$. Mole fractions for the Au_2Cl_2 species are substantially lower. The much higher mole fractions ($\sim 10^{-40}$ to $\sim 10^{-30}$) obtained for $AuCl \cdot H_2O_n$ in the present study (Appendix) reflect the effects of solute–solvate hydration (Eqn. 1).

Very few studies have been conducted on the stability of metals, or metal chlorides, in water vapor at elevated temperatures and pressures. The metals investigated in these studies were sodium (Bischoff et al., 1986; Armellini and Tester, 1993), mercury (Barnes and Seward, 1997), copper (Xiao, 1999), and silver (Migdisov et al., 1999). These studies, except that dealing with mercury, were conducted to obtain the hydration number (stoichiometry) of the cation; Barnes and Seward (1997) investigated the effects of water vapor on mercury transport. Armellini and Tester (1993) concluded that Na has fivefold coordination between 450 and 550°C and 100 to 250 bars. The same coordination number (5) was obtained for copper by Xiao (1999), whereas Migdisov et al. (1999) concluded that silver has fourfold coordination. On the basis of the results of the present study, gold has a variable coordination number, which decreases from 6 at 300°C to 4 at 360°C. Although this variation in coordination seems unusual, Seward et al. (1996) reported a similar dependence of coordination number on temperature (25 to 350°C) for aquated Ag^+.

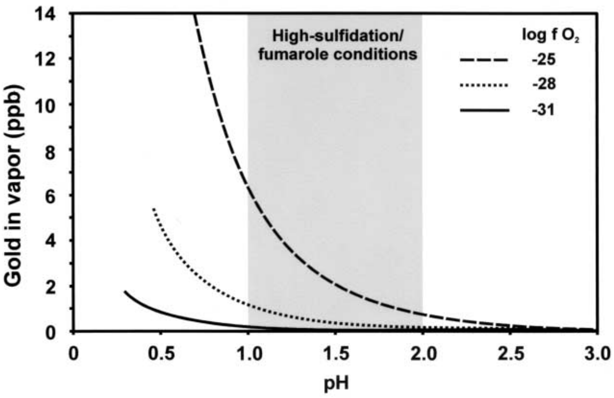

Fig. 6. Plot of calculated gold concentration (ppb) as a function of pH at 300°C. The lines correspond to log f_{O_2} values of −31 ($H_2S\text{-}SO_2$ buffer), −28 (Ag-AgCl buffer; Gammons and Williams-Jones, 1997) and −25. The shaded area represents pH conditions for a high-sulfidation ore deposit environment. The concentration of gold found in active fumaroles, when transported as a hydrated Au-Cl species, can only be explained by very high oxygen fugacities, as our calculations suggest. This implies that $AuCl \cdot (H_2O)_5$ might not be the only gold species present in the vapor.

4.4. Geological Implications

The underlying motivation of the present study was to evaluate the potential of aqueous vapor to transport sufficient gold to form economic deposits. To do this with the experimental data presented above, we need to identify an ore-forming environment in which the vapor phase is dominant and conditions are favorable for the formation of stable hydrated gold chloride gas species, i.e., temperature is moderate, pH is low, f_{O_2} is very high, and chlorinity is relatively high. The obvious candidate is the so-called acid-sulfate or high-sulfidation epithermal environment. Mineralization in this environment is characterized by temperatures typically ≤300°C, alteration/mineralization assemblages that reflect pH <2 (e.g., presence of vuggy silica) and log f_{O_2} values ≥ −28 at 300°C (e.g., the occurrence of hypogene chloragyrite and native silver) (cf. Stoffregen, 1987; Giggenbach, 1992; Arribas, 1995; Gammons and Williams-Jones, 1997; Cooke and Simmons, 2000). The salinity of the inferred orthomagmatic vapor component of the ore fluid is approximately 2 wt% NaCl equivalent (Arribas, 1995).

On the basis of the above observations, we calculated the solubility of gold at 300°C in a vapor containing 2 wt% NaCl equiv., pH values from 1 to 2 and log f_{O_2} values from −25 to −31. This was accomplished by first calculating the fugacity of HCl over the coexisting aqueous NaCl solution by using the HCh thermodynamic program (Shvarov and Bastrakov, 1999) and data for the HCl gas species from Naumov et al. (1974), then substituting the calculated f_{HCl} into Eqn. 17. The resulting fugacities are plotted in Figure 6, from which it is apparent that concentrations approaching those of gold condensates are found only at very low pH and high f_{O_2}. For example, at a pH of 2, the gold concentration in the vapor is 0.06 ppb for a log oxygen fugacity of −28, but it climbs to 0.6 ppb at a pH of 1 and the same f_{O_2}, and 3.5 ppb if log f_{O_2} is increased to −25.

A rough estimate of the time required to form an epithermal gold deposit (e.g., Nansatsu, Japan, which contains 36 tonnes of Au; Hedenquist et al., 1994) from a fluid containing the above concentrations of gold can be estimated by use of the data on HCl fluxes from active volcanoes. At a mean HCl flux of 350 tonnes per day and a gold concentration of 1.2 ppb (with a pH = 1 and log $f_{O_2} = -28$), the hydrothermal system could form a 36-tonne deposit in 238 ka. The time would be reduced to 167 ka if the flux were increased to 500 tonnes of HCl. Similar calculations that used a higher log f_{O_2} of −25, which would produce a gold concentration in the vapor of 6.6 ppb, reduce the formation times to 43 ka and 30 ka for fluxes of 350 and 500 tonnes per day of HCl, respectively. These times are within the 1 to 2 million year lifespan for hydrothermal systems, such as Steamboat Springs, Nevada (Silberman et al., 1979), and time frames predicted by Cathles et al. (1997), who calculated that a near-surface intrusion can maintain a temperature of 300°C for a maximum of 300 ka.

Natural fumaroles, such as those found at Colima (Taran et al., 2000), Galeras (Goff et al., 1994), Momotombo (Gemmell, 1987), and Mount St. Helens (Bernard and Le Guern, 1986) typically contain concentrations of gold >0.1 ppb and frequently as high as several parts per billion. Therefore, it is unlikely that $AuCl \cdot (H_2O)_{5\text{-}3}$ is the dominant Au species in this environment. Considering the significant fluxes of H_2S and SO_2 from these volcanoes (≤500 tons/day), the high concentration of H_2S in some gold-bearing, vapor-rich fluid inclusions (Ulrich et al., 1999), and the ability of H_2S to form strong complexes with gold in the liquid phase (Seward, 1973; Benning and Seward, 1996), it is likely that H_2S also plays an important role in the vapor transport of gold. In the future, we plan to conduct experiments designed to evaluate the contribution that H_2S complexes play in the transport of gold by the vapor phase.

5. CONCLUSIONS

We have shown experimentally that appreciable concentrations of Au can be transported in chloride-bearing water vapor and that these concentrations are 20 to 30 orders of magnitude greater than those of the water-free system. The reason for this is the formation of a hydrated gold–chloride species via a reaction of the type

$$Au^{gas} + m \cdot HCl^{gas} + n \cdot H_2O^{gas} = AuCl_m \cdot (H_2O)_n^{gas} + \frac{m}{2} \cdot H_2{}^{gas}.$$

The gold–chlorine ratio of the species is 1:1 (e.g., AuCl), and the overall stoichiometry is interpreted to be $AuCl \cdot (H_2O)_5$, $AuCl \cdot (H_2O)_4$, and $AuCl \cdot (H_2O)_3$ at temperatures of 300, 340, and 360°C, respectively. Interestingly, gold solubility is retrograde, i.e., it decreases with increasing temperature, which may be due to the lower stability of hydrated complexes with smaller hydration numbers.

At conditions of temperature, pH, and f_{O_2} associated with the formation of high sulfidation epithermal deposits, our data on the solubility of Au at elevated temperatures indicate that water vapor with chlorinities typical of the orthomagmatic vapor phase (the potential ore fluid) can transport low, but significant, concentrations (<0.5 ppb) of Au. Under ideal conditions, this water could theoretically form an economic gold deposit in as little as 30 ka. However, given the evidence of much higher concentrations of Au in volcanic gases and fluid inclusions, it seems more likely that other vapor species, such as H_2S, will play a more important role in the transport of gold by water vapor.

Acknowledgments—This research was made possible through grants from NSERC and FCAR to A.E.W.-J. and a Max Stern Recruitment Fellowship from McGill University to S.M.A. We thank G. Kennedy, École Polytechnique, Montreal, for performing instrumental neutron activation analysis. A review by J. R. Clark helped improve an early version of the manuscript. Comments and constructive criticism by I.-M. Chou, W. Bourcier, and J. B. Fein were also helpful.

Associate editor: J. B. Fein

REFERENCES

Armellini F. J. and Tester J. W. (1993) Solubility of sodium chloride and sulfate in sub- and supercritical water vapor from 450–550°C and 100–250 bars. *Fluid Phase Equilibria* **84,** 123–142.

Arribas A. Jr. (1995) Characteristics of high-sulfidation epithermal deposits, and their relation to magmatic fluid. In *Magmas, Fluids, and Ore Deposits* (ed. J. F. H. Thompson), Vol. 13, pp. 419–454. Mineralogical Association of Canada.

Barnes H. L. and Seward T. M. (1997) Geothermal systems and mercury deposits. In *Geochemistry of Hydrothermal Ore Deposits* (ed. H. L. Barnes), 3rd ed., pp. 699–736. Wiley.

Benning L. G. and Seward T. M. (1996) Hydrosulphide complexing of Au(I) in hydrothermal solutions from 150 to 400°C and 500 to 1500 bars. *Geochim. Cosmochim. Acta* **60,** 1849–1971.

Bernard A. and Le Guern F. (1986) Condensation of volatile elements in high temperature gases at Mt. St. Helens. *J. Volcanol. Geotherm. Res.* **28,** 91–105.

Biltz W., Fischer W., and Juza R. (1928) Über die pneumatolytische Überführung von gold durch chlor. *Z. Anorg. Allgem. Chem.* **176,** 121–142.

Bischoff J. L., Rosenbaure R. J., and Pitzer K. S. (1986) The system NaCl-H_2O: Relations of vapor–liquid near the critical temperature of water and of vapor–liquid–halite from 300 to 500°C. *Geochim. Cosmochim. Acta* **50,** 1437–1444.

Cathles L. M., Erendi A. H. J., and Barrie T. (1997) How long can a hydrothermal system be sustained by a single intrusive event? *Econ. Geol.* **92,** 766–771.

Cooke D. R. and Simmons S. F. (2000) Characteristics and genesis of epithermal gold deposits. In *Gold in 2000* (eds. S. G. Hagemann and P. E. Brown). *Rev. Econ. Geol.* **12,** 221–244.

Drummond S. E. and Ohmoto H. (1985) Chemical evolution and mineral deposition in boiling hydrothermal systems. *Econ. Geol.* **80,** 126–147.

Fischer W. and Biltz W. (1928) Über die verwantschaft von chlor und anderen halogenen zum golde. *Z. Anorg. Allgem. Chem.* **176,** 81–111.

Gammons C. H. and Williams-Jones A. E. (1997) Chemical mobility of gold in the porphyry–epithermal environment. *Econ. Geol.* **92,** 45–59.

Gemmell J. B. (1987) Geochemistry of metallic trace elements in fumarole condenstates from Nicaraguan and Costa Rican volcanoes. *J. Volcanol. Geotherm. Res.* **33,** 161–181.

Getahun A., Reed M. H., and Symonds R. B. (1996) Mount St. Augustine Volcano fumarole wall rock alteration: Mineralogy, zoning, composition and numerical models of its formation process. *J. Volcanol. Geotherm. Res.* **71,** 73–107.

Giggenbach W. F. (1992) Magma degassing and mineral deposition in hydrothermal systems along converging plate boundaries. *Econ. Geol.* **87,** 1927–1944.

Goff F., Stimac J. A., Larocque A. C. L., Hulen J. B., McMurtry G. M., Adams A. I., Roldan M. A., Trujillo P. E. Jr., Counce D., Chipera S. J., Mann D., and Heizler M. (1994) Gold degassing and deposition at Galeras Volcano, Colombia. *GSA Today* **4,** 241, 244–247.

Hager J. P. and Hill R. B. (1970) Thermodynamic properties of the vapor transport reactions in the Au-Cl system by a transpiration-mass spectrometric technique. *Metall. Trans.* **1,** 2723–2731.

Hedenquist J. W. (1995) The ascent of magmatic fluids: Discharge versus mineralization. In *Magmas, Fluids, and Ore Deposits* (ed. J. F. H. Thompson), Vol. 13, pp. 263–290. Mineralogical Association of Canada.

Hedenquist J. W. and Lowenstern J. B. (1994) The role of magmas in the formation of hydrothermal ore deposits. *Nature* **370,** 519–526.

Hedenquist J. W., Matsuhisa Y., Izawa E., White N. C., Giggenbach W. F., and Aoki M. (1994) Geology geochemistry, and origin of high sulidation Cu-Au mineralization in the Nansatsu District, Japan. *Econ. Geol.* **89,** 1–30.

James S. E. and Hager J. P. (1978) High temperature vaporization chemistry in the gold–chlorine system including formation of vapour complex species of gold and silver with copper and iron. *Metall. Trans. B* **9B,** 501–508.

Kestin J., Sengers J. V., Kamgar-Parsi B., and Levelt Sengers J. M. H. (1984) Thermophysical properties of fluid H_2O. *J. Phys. Chem. Ref. Data* **13,** 175–183.

Landsberg A. and Hoatson C. L. (1970) The kinetics and equilibria of the gold–chlorine system. *J. Less Common Metals* **22,** 327–339.

Marshall W. L. (1972) A further description of complete equilibrium constants. *J. Phys. Chem.* **76,** 720–731.

Migdisov A. A., Suleimenov O. M., and Alekhin Y. V. (1998) Experimental study of polysulfane stability in gaseous hydrogen sulfide. *Geochim. Cosmochim. Acta* **62,** 2627–2635.

Migdisov A. A., Williams-Jones A. E., and Suleimenov O. M. (1999) The solubility of chlorargyrite (AgCl) in water vapor at elevated temperatures and pressures. *Geochim. Cosmochim. Acta* **63,** 3817–3827.

Naumov G. B., Ryzhenko B. N., and Khodakovskii I. L. (1974) *Handbook of Thermodynamic Data.* NTIS.

Robie R. A. (1966) Thermodynamic properties of minerals. In *Handbook of Physical Constants* (ed. S. P. Clark Jr.), pp. 437–458. Memoir 97. Geological Society of America.

Ruaya J. R. and Seward T. M. (1987) The ion-pair constant and other thermodynamic properties of HCl up to 350°C. *Geochim. Cosmochim. Acta* **37,** 379–399.

Sandler S. I. (1989) *Chemical and Engineering Thermodynamics.*Wiley.

Seward T. M. (1973) Thio complexes of gold and the transport of gold in hydrothermal ore solutions. *Geochim. Cosmochim. Acta* **51,** 121–130.

Seward T. M., Henderson C. M. B., Charnock J. M., and Dobson B. R. (1996) An X-ray absorption (EXAFS) spectroscopic study of aquated Ag^+ in hydrothermal solutions to 350°C. *Geochim. Cosmochim. Acta* **60,** 2273–2282.

Shvarov Y. V. and Bastrakov E. N. (1999) *HCh, a Software Package for Geochemical Equilibrium Modeling: User's Guide.* Record 1999/25. Australian Geological Survey Organisation.

Silberman M. L., White D. E., Keith T. E. C., and Dockter R. D. (1979) Duration of hydrothermal activity at Steamboat Springs, Nevada, from ages of spatially associated volcanic rocks. Professional Paper 458. U.S. Geological Survey.

Spycher N. F. and Reed M. H. (1989) Evolution of a Broadlands-type epithermal ore fluid along alternative P-T paths: Implications for the transport and deposition of base, precious, and volatile metals. *Econ. Geol.* **84,** 328–359.

Stoffregen R. E. (1987) Genesis of acid-sulfate alteration and Au-Cu-Ag mineralization at Summitville, Colorado. *Econ. Geol.* **82,** 1575–1591.

Symonds R. B., Rose W. I., Reed M. H., Lichte F. E., and Finnegan D. L. (1987) Volatilization, transport and sublimation of metallic and non-metallic elements in high temperature gases at Merapi Volcano, Indonesia. *Geochim. Cosmochim. Acta* **51,** 2083–2101.

Symonds R. B. and Reed M. H. (1993) Calculation of multicomponent chemical equilibria in gas–solid–liquid systems; calculation methods, thermochemical data, and applications to studies of high-temperature volcanic gases with examples from Mount St. Helens. *Am. J. Sci.* **293,** 758–864

Symonds R. B., Rose W. I., Bluth G. J. S., and Gerlach T. M. (1994) Volcanic-gas studies: Methods, results and applications. In *Volatiles in Magmas* (eds. M. R. Carroll and J. R. Holloway), pp. 1–66. Mineralogical Society of America.

Tagirov V. K., Makarov V. A., and Brukvin V. A. (1993) Vapor composition and pressure over chlorides of silver and gold. *Metalli* **5,** 67–71.

Tagirov B. R., Zotov A. V., and Akinfiev N. N. (1997) Experimental study of dissociation of HCl from 350 to 500°C and 500 to 2500 bars; thermodynamic properties of $HCl_o^{(aq)}$. *Geochim. Cosmochim. Acta* **61,** 4267–4280.

Taran Y. A., Bernard A., Gavilanes J.-C., and Africano F. (2000) Native gold in mineral precipitates from high-temperature volcanic gases of Colima volcano, Mexico. *Appl. Geochem.* **15,** 337–346.

Ulrich T., Günther D., and Heinrich C. A. (1999) Gold concentrations of magmatic brines and the metal budget of porphyry copper deposits. *Nature* **399,** 676–678.

Xiao Z. (1999) Experimental and theoretical studies of the solubility of copper in liquid and vapor in the system NaCl-HCl-H_2O. Ph.D. dissertation. McGill University.

Zotov A. V., Baranova N. N., Dar-ina T. G., and Bannykh L. N. (1990) Solubility of gold in aqueous chloride fluids at 350–500°C, 500–1500 atm pressure and thermodynamic properties of $AuCl_-^2$ (sol) up to 750°C and 5000 atm. *Geokhimiya* **7,** 979–987.

APPENDIX

Table A1. Fugacities and mole fractions of gas species at 300°C and a logf_{O_2} of −21. The values of log$f$AuCl$_m$ · (H$_2$O)$_m$ were subjected to a Poynting correction that was typically about 0.12 bars.

log f_{H_2O} (bar^{-1})	log f_{HCl} (bar^{-1})	log $X_{AuCl_m \cdot (H_2O)_n}$	log $f_{AuCl_m \cdot (H_2O)_n}$ (bar^{-1})
1.80	−2.17	−11.37	−9.34
1.80	−2.18	−10.94	−8.90
1.80	−2.18	−11.73	−9.69
1.81	−2.71	−11.49	−9.44
1.82	−2.18	−10.89	−8.83
1.82	−2.41	−11.32	−9.26
1.82	−2.42	−11.79	−9.72
1.82	−1.92	−10.74	−8.67
1.83	−1.82	−10.65	−8.57
1.83	−2.95	−12.05	−9.98
1.83	−1.60	−10.15	−8.07
1.83	−1.16	−10.01	−7.93
1.83	−2.31	−10.22	−8.14
1.83	−2.83	−11.46	−9.38
1.80	−2.18	−10.94	−8.90
1.82	−2.18	−10.89	−8.83
1.80	−2.17	−11.37	−9.34
1.46	−2.00	−11.48	−9.92
1.54	−2.00	−11.46	−9.81
1.68	−2.00	−11.14	−9.30
1.50	−2.00	−11.68	−10.08
1.57	−2.00	−11.78	−10.09
1.82	−1.92	−10.74	−8.67
1.83	−1.82	−10.65	−8.57
1.44	−1.19	−11.64	−10.12
1.61	−1.19	−12.09	−10.35
1.77	−1.19	−10.80	−8.82
1.59	−1.18	−12.08	−10.36
1.71	−1.18	−10.91	−9.02
1.68	−1.18	−12.40	−10.55
1.62	−1.18	−11.90	−10.14
1.74	−1.18	−10.71	−8.77

Table A2. Fugacities and mole fractions of gas species at 340°C and a logf_{O_2} of −20. The values of logf_{AuCl_m} · (H$_2$O)$_n$ were subjected to a Poynting correction that was typically about 0.19 bars.

log f_{H_2O} (bar^{-1})	log f_{HCl} (bar^{-1})	log $X_{AuCl_m \cdot (H_2O)_n}$	log $f_{AuCl_m \cdot (H_2O)_n}$ (bar^{-1})
2.01	−1.25	−11.10	−8.74
2.02	−1.19	−12.26	−9.90
2.02	−2.71	−13.29	−10.92
2.02	−2.26	−11.90	−9.53
2.02	−1.80	−12.66	−10.29
2.02	−1.18	−10.92	−8.56
2.02	−0.78	−10.00	−7.64
2.02	−1.39	−11.74	−9.37
2.02	−1.32	−11.71	−9.34
2.02	−0.97	−12.09	−9.72
2.02	−0.77	−10.17	−7.80
2.02	−0.61	−11.38	−9.02
1.91	−1.19	−12.43	−10.27
1.81	−1.19	−12.25	−10.25
1.96	−1.19	−11.69	−9.44
1.87	−1.19	−12.15	−10.06
1.97	−1.18	−12.11	−9.85
1.69	−1.18	−12.41	−10.57

Table A3. Fugacities and mole fractions of gas species at 360°C and a logf_{O_2} of −19. The values of log$f_{AuCl_m} \cdot (H_2O)_n$ were subjected to a Poynting correction that was typically about 0.17 bars.

log f_{H_2O} (bar^{-1})	log f_{HCl} (bar^{-1})	log $X_{AuCl_m \cdot (H_2O)_n}$	log $f_{AuCl_m \cdot (H_2O)_n}$ (bar^{-1})
2.04	−1.75	−11.78	−9.42
2.04	−1.32	−12.26	−9.89
2.04	−1.66	−11.53	−9.16
2.04	−0.92	−11.81	−9.44
2.04	−1.18	−11.43	−9.05
2.04	−0.86	−10.79	−8.42
2.04	−2.32	−12.84	−10.46
2.05	−2.28	−12.30	−9.90
2.04	−2.06	−11.36	−8.98
2.05	−1.93	−10.88	−8.48
1.95	−1.92	−11.64	−9.44
1.82	−1.92	−10.76	−8.75
1.86	−1.91	−10.85	−8.79
1.67	−1.91	−10.95	−9.15
1.76	−1.91	−11.54	−9.62
1.59	−1.91	−11.39	−9.70
1.44	−1.91	−12.14	−10.63